Studies of electronic structure of ZnO grain boundary and its proximity by using spatially resolved electron energy loss spectroscopy

H. C. Ong[a)]
Department of Physics, The Chinese University of Hong Kong, Shatin, Hong Kong

J. Y. Dai
Department of Applied Physics, The Hong Kong Polytechnic University, Hong Kong

G. T. Du
State Key Laboratory on Integrated Optoelectronics, Jilin University, People's Republic of China

(Received 11 December 2001; accepted for publication 2 May 2002)

The low electron energy loss and complex dielectric functions of an arbitrary grain boundary and its proximity in ZnO thin films have been studied by using the spatially resolved electron energy loss spectroscopy. The critical point parameters have been determined by fitting the dielectric functions simultaneously with analytical line shape model. Gradual changes have been observed in the dielectric functions spectra. The critical points are found to redshift and then blueshift when the electron beam scanned across the grain boundary, which suggest the distinctive electronic structure not only of the grain boundary but also of the depletion region. In addition, comparison has been made between the experiment and the recent theoretical studies to account for the interband transitions that occur in the grain boundaries. Several features predicted by the theory are qualitatively found to be consistent with our results. The presence of dangling bonds instead of bond distortion is attributed to be the major cause of defects in the grain boundaries of ZnO. © *2002 American Institute of Physics.* [DOI: 10.1063/1.1489721]

Grain boundaries (GBs) in ZnO have led to many interesting phenomena in electrical[1] as well as optical applications.[2,3] Of particular is the realization of the nonlinear electrical behavior whose primary function is to against the transient voltage surge in electronic devices.[1] In addition, the strong optical scattering that occurs at the GBs has paradoxically assisted the formation of self-assembled laser cavities.[4] Although a great deal of effort has been devoted to the research of GBs, the fundamental knowledge of the local atomic and electronic structures remains unclear. Most of the macroscopic studies have usually suffered from the lack of direct access to the electronic band structure and therefore do not examine the GBs in great detail.[1] To date, they simply indicate the presence of a depletion region at the GBs.[1] On the other hand, microscopic probes with high precision will allow the exact determination of the electronic structure with the scale down to the submicron level.[4–6] Although there have been a few studies concerning the use of electron probe to investigate the energy loss of the GBs, the majority is involved in the high-energy near-edge regime where only the unoccupied states in the conduction band are available.[5,6] The low loss region is, however, more or less disregarded. In general, the low loss study provides information of the interband transitions and may offer an alternative to examine the local electronic structure at high spatial extent.[7] Moreover, the loss function and its derivatives, such as the complex dielectric functions and optical conductivity, allow direct comparison between the theory and experiment.[7,8] Insights in these regards will complement the core-loss studies and shed light on the structure, chemistry, and electronic properties of the GBs in ZnO.

In this letter, we have studied the low electron energy loss and complex dielectric functions, $\varepsilon(E)$, of an arbitrary grain boundary in ZnO polycrystalline thin film by using the spatially resolved electron energy loss spectroscopy (EELS). The critical point (CP) parameters of the interband transitions have been determined by the analytical expressions. The variation of the CP parameters across the GB signifies the apparent changes of the electronic structure in the vicinity of the GB.[9] In addition, by comparing our experimental results with the recent theoretical studies conducted by Oba *et al.*,[10] we have qualitatively identified the interband transitions arising from the GB.

Thin films of ZnO are grown on amorphous fused silica by pulsed laser deposition in a high vacuum system. Deposition procedures have been given previously.[4] X-ray diffraction indicates a large mosaic spread of the microcrystallites and the absence of any preferential in-plane alignment. The room temperature EELS measurements are conducted in a transmission mode by using a Hitachi HF-2000 microscope operated at a beam voltage of 200 keV. The microscope is equipped with a cold field emission gun and a Gatan-666 parallel EEL spectrometer with an energy resolution of 0.5 eV determined by the full width at half maximum of the zero loss peak. This setup allows the production of a 7 Å diameter electron beam with a spatial resolution higher than 2 nm. Low energy loss spectra are line scanned from the grain to the grain boundary. The removal of the zero loss function using the Lorentizian fitting routine and the convergence and angular correction have been carried out for spectrum

a)Electronic mail: hcong@phy.cuhk.edu.hk

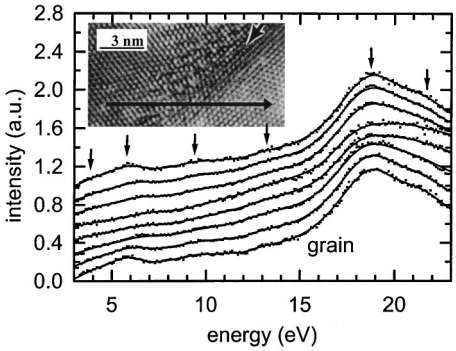

FIG. 1. The line scan of the low electron energy loss spectra across the grain boundary of ZnO. The dot lines represent the raw data while the solid lines signify the loss functions after the FFT filter. The arrows indicate the peak-like features. The inset shows the high-resolution plane-view transmission electron microscopy images illustrating the region where the measurements are taken.

correction.[7,11] The Kramers–Kronig analysis is used to convert the loss functions to the corresponding $\varepsilon(E)$.[11]

Figure 1 illustrates the energy loss spectra of ZnO line scanned across the GB after the removal of the zero loss and multiple scattering. The loss function of the grain interior exhibits essentially the bulk character and the bulk plasmon peaks are clearly visible at 18.8 eV. Several minor peaks observed at 3.86, 5.82, 9.5, 13, and 21.7 eV are determined to be the interband transitions.[12,13] Among them, the peaks at 5.82 and 9.5 eV are assigned to the transitions from the O $2p$ states to the unoccupied conduction band while the peaks at 13 and 21.7 eV are ascribed to the transitions arise from Zn $3d$ and O $2s$ levels, respectively.[13] The loss at 3.86 eV is assumed to be of defect origin that associates with the excitations from the deep states in the gap.[12] The loss function is consistent with that of Hengehold *et al.* taken by using a single crystal.[14] As the electron beam is moving towards the GB, however, the loss profile slowly changes, which corresponds to the change of the electron transitions at the GB. The profile is becoming slightly level overall and several features begin to arise. In order to clarify the difference between the energy losses of the grain and grain boundary, second derivative spectra instead of the raw data are examined. After the smoothing procedure by using the fast Fourier transform (FFT) filter, the differentiated loss spectra are presented in Fig. 2. The line spectra indicate most of the loss peaks are reducing in intensity and the features at 5.82 and 9.5 eV are changing gradually over to two prominent peaks at 7 and 10.33 eV. In addition, the peak at 21.7 eV is split

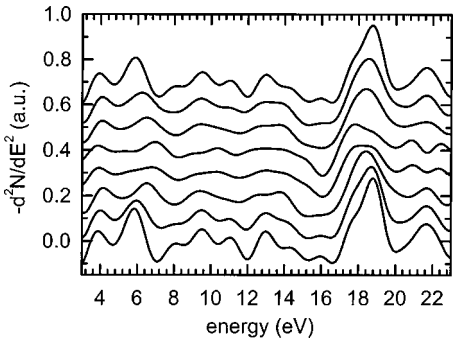

FIG. 2. The second derivative spectra derived from the corresponding loss functions.

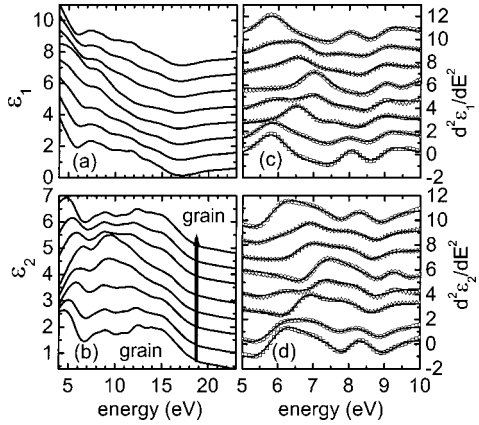

FIG. 3. The complex dielectric functions, (a) and (b), in the proximity of the ZnO grain boundary computed from the loss functions. The second-derivative dielectric functions spectra (symbols) together with the best fits (solid-line) using the analytical line shape mode, (c) and (d).

into two small peaks appear at 20.75 and 22.44 eV. The attenuation of the bulk plasmon is accompanied with the emergence of a peak at 17.74 eV, which can be attributed to the interface plasmon. The plasmon is also found to blue-shifted slightly in the GB even though it is almost completely masked by the 17.74 eV peak.

The complex dielectric functions have been determined by using the Kramers–Kronig analysis and are plotted in Figs. 3(a) and 3(b). The $\varepsilon(E)$ of the grain interior are shown to agree well with that of the bulk obtained from the reflectivity measurement.[14,15] Slight disparity is noticed although it is expected from two different methods. In the GB dielectric functions, however, notable changes have been observed with respect to that of the spectra from grain, especially at the energy range of 5–13 eV where transitions of O $2p$ and Zn $3d$ levels dominate.[9,13] In fact, most of the fine structures given in the grain spectra are being smeared out at this energy region. The intensity of the imaginary part of the dielectric functions, ε_2, is also found to increase in the GB and peak-like features are visible at 6.08, 9.22, and 11.54 eV.

It is known that $\varepsilon(E)$ corresponds to the joint density of states (JDOS) in which electron excitations will take place when both the densities of the valence and conduction states involved in the relevant transitions are significant.[16] In addition, the structure of the $\varepsilon(E)$ can be considered as a sum of contribution from all allowable transitions at the CPs, which can be analyzed in terms of the line shape expression given as[9]

$$\varepsilon(E) = C - Ae^{i\phi}(E - E_C + i\Gamma)^n \tag{1}$$

for one CP, where A, ϕ, E_c, and Γ are the amplitude, phase angle, energy position, and the line broadening. The n indicates the dimensionality of the CP. The parameters from 5 to 10 eV have been determined by fitting the second-derivative $\varepsilon(E)$ spectra simultaneously using three two-dimensional (2D) CPs and the results are summarized in Fig. 4. The shaded area is the GB. The best fits along with the second derivative spectra are illustrated in Figs. 3(c) and 3(d). The CP positions are found to remain relatively constant in the grain interior. However, they redshift slightly in the proximity of the GB and blueshift at the GB. Likewise, the ampli-

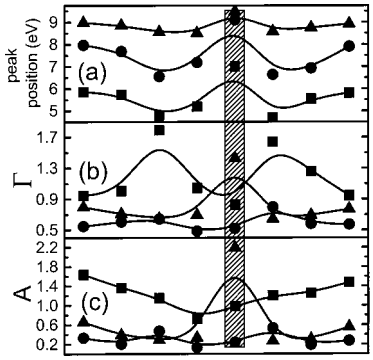

FIG. 4. The critical point peak position (a), line broadening Γ (b), and amplitude *A* (c). The square, circle, and triangle symbols represent the first, second, and third 2D critical points. The shaded area is the location of the GB.

tude and line broadening behave similarly when changes occur not only at the GB but also near the GB.

Although the origin of the redshift of CPs remains unclear, it may be attributed to the presence of a back-to-back potential barrier region in the vicinity of the GB where positive and negative charges are distributed unevenly and therefore depleted.[17] In addition, the bond distortion before reaching the GB may also give rise to such a change. Nonetheless, our results in fact indicate the electronic structure of the depletion region is quite distinct from the grain interior as well as the GB.

Finally, an attempt has been made to assign the transition processes responsible for the EEL and dielectric functions observed in the GB. Recently, Oba *et al.* have calculated the electronic structures of the GBs in ZnO using *ab initio* plane-wave pseudopotential and the first principle methods.[10] Two GB models have been considered in which the structure is either made up of small bond distortion together with dangling bonds or large bond distortion but without dangling bonds. It is shown that the DOS of GBs indeed are quite different from that of the grain with distinguishable changes observed in the general shapes of the valence and conduction bands. In particular, their calculations have illustrated that the presence of dangling bonds at the GB will not only affect the conduction band edge where most of the defect states locate, but also the resulting O $2s$ valence band. Dangling bonds broaden the O $2s$ band as well as split it into two smaller levels. Hence, their work may offer a preliminary background for us to elucidate the electronic transitions in the EEL and dielectric functions. To begin with our comparison, we first consider the entire DOS of the GBs displayed in Ref. 9. It has been shown that the valence DOS of the GBs are flatter and wider than that of the grain whereas the DOS of the conduction edge are higher. However, major changes in the valence band structure occur at the energy range of -4 to -7 eV where the transitions involve primarily of O $2p$ and Zn $3d$ states. Therefore, it is reasonable to correlate the increase of the O $2p$ and Zn $3d$ excitations to the JDOS, which results in the change of the intensity and peak position of ε_2 at 5–15 eV. This is consistent with the experiment. Likewise, the same scenario applies to the variations in the GB loss function. On the other hand, the evolution of two peaks at 20.85 and 22.44 eV in the EEL can be described by the splitting of the O $2s$ level leading to the conclusion that dangling bonds instead of bond distortion are prevailing in our GB.[10] In fact, our previous study on the second harmonic generation of ZnO thin films has indicated a significant part of the nonlinear optical output is generated by the dipoles, or dangling bonds, at the GBs,[18] which agrees with our argument.

In summary, we have mapped out the complex dielectric functions in the proximity of an arbitrary ZnO GB by using the scanning EELS and determine the CP parameters analytically. The dielectric functions of the GB are found to be quite distinct from that of the grain as well as the depletion region and this indicates observable changes of the electronic structure across the GB. Our results have been compared with the recent studies on the ZnO GBs and fair agreement is reached despite more experimental and theoretical work should be carried out. We believe the dangling bonds instead of bond distortion are the primary cause of defects in the GB.

This research was supported by the Chinese University of Hong Kong through the RGC Competitive Earmarked Research Grants (Nos. CUHK1101/99E and CUHK1157/01E), the Direct Grant (No. 2060218) and the NSFC/RGC Joint Research Scheme (No. NCUHK127/99).

[1] T. K. Gupta, J. Am. Ceram. Soc. **73**, 1817 (1990).
[2] H. Cao, Y. G. Zhao, H. C. Ong, S. T. Ho, J. Y. Dai, J. Y. Wu, and R. P. H. Chang, Appl. Phys. Lett. **73**, 3656 (1998).
[3] Z. K. Tang, G. K. L. Wong, P. Yu, M. Kawasaki, A. Ohtomo, H. Koinuma, and Y. Segawa, Appl. Phys. Lett. **72**, 3270 (1998).
[4] H. C. Ong, J. Y. Dai, K. C. Hung, Y. C. Chan, R. P. H. Chang, and S. T. Ho, Appl. Phys. Lett. **77**, 1484 (2000).
[5] N. D. Browning, H. O. Moltaji, and J. P. Buban, Phys. Rev. B **58**, 8289 (1998); N. D. Browning, J. P. Buban, H. O. Moltaji, S. J. Pennycook, G. Duscher, K. D. Johnson, R. P. Rodrigues, and V. P. Dravid, Appl. Phys. Lett. **74**, 2638 (1999).
[6] D. A. Muller, S. Subramanian, P. E. Batson, S. L. Sass, and J. Silcox, Phys. Rev. Lett. **75**, 4744 (1995); D. A. Muller, D. J. Singh, and J. Silcox, Phys. Rev. B **57**, 8181 (1998); D. A. Muller, *ibid.* **58**, 5989 (1998).
[7] H. Mullejans and R. H. French, J. Phys. D **29**, 1751 (1996).
[8] S. Kohiki, M. Arai, H. Yoshikawa, S. Fukushima, M. Oku, and Y. Waseda, Phys. Rev. B **62**, 7964 (2000); S. Atzkern, S. V. Borisenko, M. Knupfer, M. S. Golden, J. Fink, A. N. Yaresko, V. N. Antonov, M. Klemm, and S. Horn, *ibid.* **61**, 12792 (2000).
[9] P. Lautenschlager, M. Garriga, and M. Cardona, Phys. Rev. B **36**, 4813 (1987).
[10] F. Oba, S. R. Nishitani, H. Adachi, I. Tanaka, M. Kohyama, and T. Shingo, Phys. Rev. B **63**, 045410 (2001); F. Oba, I. Tanaka, S. R. Nishitani, H. Adachi, B. Slater, and D. H. F. Gay, Philos. Mag. A **80**, 1567 (2000).
[11] R. F. Egerton, *Electron Energy Loss Spectroscopy in the Electron Microscope* (Plenum, New York, 1986).
[12] P. J. Møller, S. A. Komolov, E. F. Lazneva, and E. H. Pedersen, Surf. Sci. **323**, 102 (1995).
[13] S. Bloom and I. Ortenburger, Phys. Status Solidi B **58**, 561 (1973); M. Scrocco, J. Electron Spectrosc. Relat. Phenom. **53**, 225 (1991).
[14] R. L. Hengehold, R. J. Almassy, and F. L. Pedrotti, Phys. Rev. B **1**, 4784 (1970).
[15] R. Klucker, H. Nelkowski, Y. S. Park, M. Skibowski, and T. S. Wanger, Phys. Status Solidi **45**, 265 (1971).
[16] K. Ueda, H. Yanagi, R. Noshiro, H. Hosono, and H. Kawazoe, J. Phys.: Condens. Matter **10**, 3669 (1998).
[17] V. Srikant, V. Sergo, and D. R. Clarke, J. Am. Ceram. Soc. **78**, 1935 (1995).
[18] H. Cao, J. Y. Wu, H. C. Ong, J. Y. Dai, and R. P. H. Chang, Appl. Phys. Lett. **73**, 572 (1998).